fibers

MDPI

Article

Physical and Mechanical Characterization of Flax Fibers: From Elementary Fiber to Yarn

Wafa Mahjoub [1,2,*] and Omar Harzallah [1,2]

[1] Laboratoire de Physique et Mécanique Textiles (LPMT, UR 4365), Université de Haute Alsace, 11 Rue Alfred Werner, 68093 Mulhouse, France; omar.harzallah@uha.fr
[2] Université de Strasbourg, 67081 Strasbourg, France
* Correspondence: wafa.mahjoub@uha.fr

Highlights

What are the main findings?

- A multiscale experimental analysis of flax was conducted, from elementary fibers to yarns.
- Mechanical performance was found to decrease across scales due to fiber misalignment and variability.
- Longer bundles and finer yarns exhibited significantly higher modulus and tenacity, primarily due to improved fiber alignment and structural homogeneity.

What are the implications of these findings?

- This study offers an industrially relevant framework for optimizing flax yarn performance by controlling fiber alignment through dry spinning and GN combing.
- The results support improved processing strategies for scalable, consistent, and sustainable natural fiber textile production.

Abstract

This study presents a multiscale characterization of flax fibers, from elementary fibers to technical bundles and yarns, to elucidate how fiber scale attributes influence yarn mechanics. Four yarn counts (111.11 tex, 100 tex, 90.9 tex, and 83.33 tex) were produced via dry spinning, and tensile testing performed at each structural level. The results revealed a progressive decline in a specific modulus from elementary fibers (1.09 $\pm$ 0.62 N/tex) to short bundles (14.41 $\pm$ 9.59 N/tex), primarily due to fiber misalignment. Post hoc analysis confirmed that finer yarns (83.33 tex) exhibited higher stiffness (7.32 $\pm$ 1.69 N/tex, $p < 0.001$), attributed to advanced processing (GN4 combing). These findings highlight the critical role of fiber length and alignment in optimizing flax yarns for high-performance textiles.

Keywords: flax; multiscale characterization; specific modulus; fineness; length

check for updates

Academic Editor: Martin J. D. Clift

Received: 9 May 2025
Revised: 6 June 2025
Accepted: 26 June 2025
Published: 30 June 2025

Citation: Mahjoub, W.; Harzallah, O. Physical and Mechanical Characterization of Flax Fibers: From Elementary Fiber to Yarn. *Fibers* **2025**, *13*, 87. https://doi.org/10.3390/fib13070087

Copyright: © 2025 by the authors. Licensee MDPI, Basel, Switzerland. This article is an open access article distributed under the terms and conditions of the Creative Commons Attribution (CC BY) license (https://creativecommons.org/licenses/by/4.0/).

1. Introduction

Flax (*Linum usitatissimum* L.) is a lignocellulosic bast fiber known for its sustainability, low density, high stiffness, and biodegradability. These qualities make it an increasingly attractive material in both textile and technical applications [1–3]. However, to fully capitalize on its potential in spinning processes, it is essential to understand how its physical and mechanical properties at different scales influence its tensile behavior in yarn form [4,5].

Flax fiber has a multiscale structure that can be described at four main levels: macroscopic, mesoscopic, microscopic, and nanoscopic. At the macroscopic scale, yarn is considered a final assembled product ready for use in textile applications. At the mesoscopic scale, flax appears as bundles of technical fibers: groups of 10 to 40 elementary fibers that are bound together in the phloem region of the plant stem. These bundles typically extend over several tens of centimeters, and their size and structure depend on the plant variety and its harvesting stage [6].

At the microscopic scale, the elementary fiber is an individual cell with a polygonal cross-section and lengths ranging from 6 to 80 mm [7]. These fibers are held together in bundles by a pectin-rich middle lamella. Their polygonal shape is thought to improve spatial packing in the plant stem. A key feature of the elementary fiber is the lumen, a central hollow channel whose size can vary along the fiber and may influence water movement during plant growth, as well as the mechanical properties after harvest [8].

At the nanoscopic scale, the flax cell wall consists of concentric layers of cellulose microfibrils embedded in a matrix of hemicellulose, lignin, and pectin [7]. The orientation and helical arrangement of these microfibrils contribute to the fiber's anisotropic mechanical behavior. This nanoscale architecture plays a crucial role in determining the stiffness and strength of the fiber at larger scales.

The choice of spinning process depends on the fiber physical properties and, in particular, the fiber length. In conventional spinning, two main categories are distinguished: short fiber spinning (cotton type) and long fiber spinning (wool type).

Spinning flax fibers involves several mechanical processing steps such as retting, scutching, and hackling [9]. These processes break down the raw material, separate the fibers, and align them for spinning. During this transformation, the inherent variability in fiber morphology and the presence of discontinuities (often linked to leaf insertion points along the stem) can weaken the structure. These discontinuities tend to act as weak points under tensile stress [10]. Nevertheless, this study does not focus on this phenomenon, which is related to the microscopic and nanoscopic scales.

Following initial processing, the fibers undergo parallelization, drafting, and twisting, which are carried out using either wet or dry spinning methods [11,12].

Dry spinning is typically employed for coarser yarns used in heavier fabrics. In this process, short flax tow undergoes limited carding and drafting without the aid of moisture, preserving the fiber's natural texture but restricting drafting due to the low extensibility of flax. In this process, drafting improves sliver fineness and length by promoting the cleavage of coarse technical fiber bundles into finer ones [13]. A semiwet variant introduces minimal water to improve fiber cohesion during spinning while maintaining ecological efficiency.

Wet spinning is the preferred method for producing fine and high-quality yarns. This process uses long, combed flax fibers (line flax or filasse), which undergo precise preparation and ribbon formation. Fibers are immersed in hot water before drafting to enhance inter-fiber slippage. Spinning is performed in a moist state, enabling high draft ratios and resulting in finer and more regular yarns. Although this method provides superior yarn quality, its intensive water usage raises environmental concerns.

In this study, dry spinning was employed to produce the four yarns tested. While substantial research has focused on flax for use in composites [14,15], fewer studies have explored yarn properties from a multiscale perspective.

Our aim is to fill this gap by providing a detailed physical and mechanical characterization of flax at three levels: the elementary fiber, the technical fiber bundle, and the yarn. We used one flax variety to reduce variability and produced four yarns with different

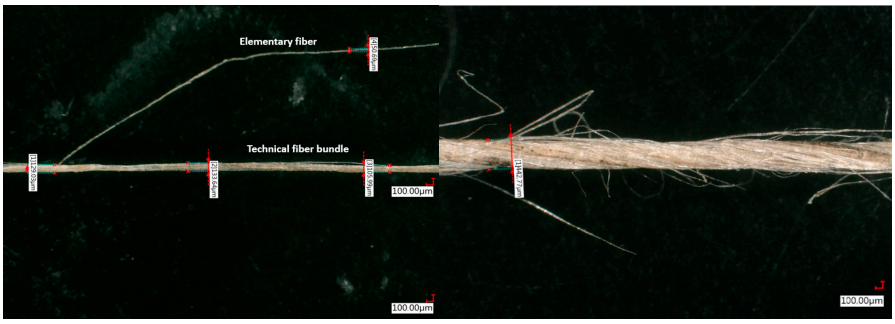
counts and twists. We measured morphological properties like fineness and length along with mechanical properties such as tenacity (N/tex) and specific modulus (N/tex).

Importantly, the dry spinning process was carefully selected and optimized, as it plays a critical role in fiber alignment and bundle integrity—key factors influencing yarn performance. While the spinning process is industrially standard, the originality of this work lies in its integrated, cross-scale analysis that links microstructural organization to the final mechanical performance of the yarn. By comparing results across scales, we aim to better understand how flax fibers influence yarn properties. Our ultimate goal is to contribute to a deeper understanding of the physical and mechanical behavior of flax fibers.

2. Materials and Methods

To minimize the influence of genetic variability on the results, all flax fibers used in this study were sourced from a single batch of industrially processed textile flax cultivated in northern France. While the specific cultivar name, harvest year, and detailed agronomic parameters were not provided by the supplier, all samples originated from the same production lot. The flax was subjected to standardized industrial processing, including field retting, mechanical scutching, and hackling, prior to testing.

This study focused on the physical and mechanical characterization of flax fibers at three structural scales: elementary fibers, technical fiber bundles, and yarns. Flax exhibits a hierarchical structure, with elementary fibers assembling into technical bundles, which are subsequently processed into yarns. A representative microscopic image illustrating both the individual elementary fibers and their aggregation into technical bundles and yarns is provided in Figure 1 to support this multiscale structural description.



(**a**) (**b**)

Figure 1. Micrograph illustrating (**a**) elementary fibers and technical bundle (**b**) yarn structures.

For each scale, specific protocols were established to ensure representative and reproducible measurements. Elementary fibers were manually extracted from the technical bundles.

Technical fiber bundles were sorted by length using the Schlumberger comb sorter (Figure 2).



Figure 2. Schlumberger comb sorter.

All the samples were conditioned under standard atmospheric conditions (20 ± 2 °C and 65 ± 2% RH) for at least 24 h prior to testing (ISO 135/2005).

2.1. Yarn Production

The flow chart of the flax spinning process is shown in Figure 3. Flax raw material was first machine-cracked and then drafted through four sequential gill drafting frames (GN1, GN2, GN3 and GN4) equipped with combs. The density of the gill drafting frames (number of points or needles on moving frames) increases progressively in order to gradually improve fiber control and alignment during drafting. The slivers exiting the final gill were transformed into a yarn product on a dry spinning frame. Four different yarn counts (111.11 tex, 100 tex, 90.9 tex, and 83.33 tex) were then produced by adjusting drafting and twist parameters.

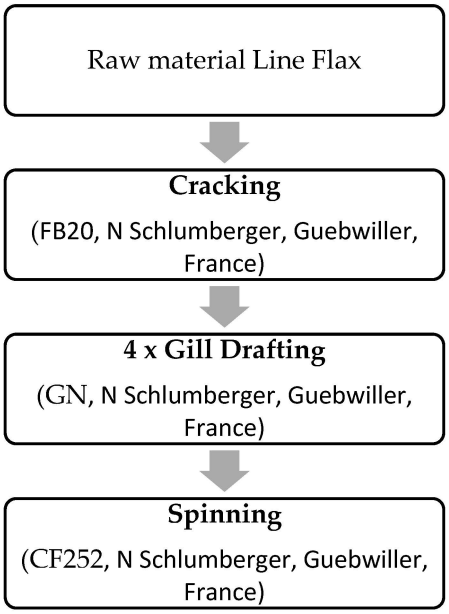


Figure 3. The flow chart of the flax fiber spinning process.

Yarn regularity, defined as mass variation per unit length along the yarn, was analyzed using a Zweigle capacitive regularity tester (Zweigle GmbH, Reutlingen, Germany). Sensor size was selected based on yarn fineness according to the manufacturer's guidelines. Testing conditions were standardized at 100 m/min for 5 min to ensure reproducibility. Key metrics for the yarn regularity characterization included the coefficient of variation (CV%) and imperfection markers (thick places: +50% threshold, thin places: −50% threshold, and neps: +200% threshold).

2.2. Physical Characterization

2.2.1. Fiber Length Distribution

Flax fiber length [16] is a key physical property that significantly influences its performance during spinning. For example, before the drafting process, it is important to study the fiber length distribution in a sliver. This distribution indicates the optimal distance between drafting rollers. Incorrect roller spacing can lead to either floating fibers or fiber breakage. Therefore, accurate knowledge of fiber length distribution is essential for producing uniform yarn quality.

In this study, the fiber length distribution was assessed according to ASTM D1440 and ISO 6989 standards using the Almeter Peyer texLab AL100 device (Siegfried Peyer AG, Zofingen, Switzerland) [17]. Almeter analysis uses a capacitive measurement system

based on the fiber beard method. For each measurement, sample masses ranged between 100 and 150 g. Three manual pulls were conducted on a black table, followed by transfer to the preparatory machine "Peyer texLab FL 100" for initial fiber beard preparation.

This beard was repositioned on the carriage using manual clamps, ensuring the tailing of each sample was drawn first, effectively straightening the fibers. Then, the device calculates key parameters: Hauteur (H), representing the mean fiber length weighted by the fiber cross-section, and Barbe (B), representing the mean length weighted by the fiber weight. It also provided the coefficient of variation (CvH% and CvB%) reflecting the variability in the H and B values determined from the distributions of the fiber cross-section and the fiber weight, respectively.

Determination of the Hauteur (H) and Barbe (B) values is performed, respectively, according to Equations (1) and (2):

$$Barbe\ (B) = \frac{\sum m_i \times l_i}{\sum m_i} \quad (1)$$

$$Hauteur\ (H) = \frac{\sum t_i \times l_i}{\sum t_i} \quad (2)$$

where:

mi: Mass of fiber bundles per class (mg).

li: Length corresponding to the class center of fiber bundles (mm).

ti: Mass per unit length (tex).

The Almeter device also provides the tuft (fibrogram), a graphical representation of the fiber length distribution within a sample (Figure 4). From the tuft, several key length parameters are determined graphically by drawing tangents at characteristic points [18].

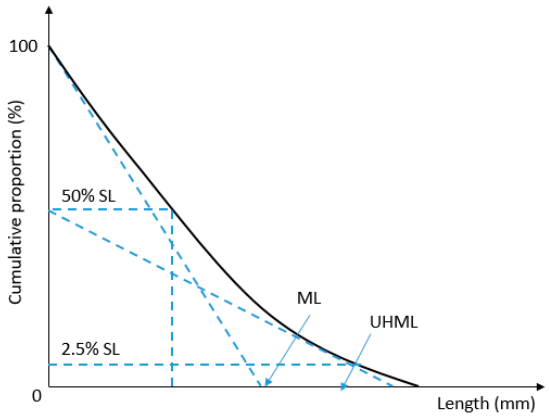


Figure 4. Tuft (fibrogram).

Mean length (ML) is obtained by drawing a tangent from the 100% fiber point and extrapolating it to the length axis. A tangent drawn from the 50% of fibers and extrapolated to the length axis indicates the upper half mean length (UHML), which indicates the average length of the longer half of the fibers. These two parameters are used to classify flax fibers according to fiber length and to assess the length uniformity within the batch through the uniformity index (UI%):

$$UI\% = 100 \times \frac{ML}{UHLM} \quad (3)$$

For this study, three length intervals were defined according to the tuft fibrogram parameters, UHML and ML:

- Short fibers: Technical fiber bundles with lengths shorter than ML.

- Medium fibers: Bundles with lengths between ML and UHML.
- Long fibers: Bundles with lengths longer than UHML.

This classification enables a detailed analysis of fiber properties and performance across distinct length categories, facilitating targeted evaluation of fiber quality within the sample.

2.2.2. Fineness

Fineness was assessed using two methods: the vibroscopic method (ASTM D1577/ISO 1973) and the air flow method (ISO 2370:1980). Technical bundles were classified into length classes using the Schlumberger comb sorter, before the fineness measurements with the vibroscope.

Textechno Vibromat ME and Favimat devices (Textechno Herbert Stein GmbH & Co. KG, Mönchengladbach, Germany) measure the fineness of either elementary fibers or fiber bundles [19].

An electroacoustic sinusoidal vibration excites the fiber, and the resonance frequency is detected using an optoelectronic sensor. The fiber fineness is then calculated, based on the resonance condition, taking into account the testing length, the pre-tensioning force, and the resonance frequency of the fiber. The fineness (in dtex) is calculated using the following relationship:

$$T = \frac{Fv\ 10^{11}}{4\ f^2 L^2} \tag{4}$$

where:

T: Fineness (dtex).

Fv: Pre-tensioning force (cN).

f: Resonance frequency (Hz).

L: Testing length (mm).

The air flow method estimates fineness indirectly via the Standard Fineness Index (SFI) using a Carman–Kozeny equation. This approach relates air flow resistance through a fiber plug to its specific surface area:

$$R = \frac{Q}{\Delta P} = \frac{S\varepsilon^2}{K_0\ \eta A^2 (1-\varepsilon^2)} \tag{5}$$

where:

R: Air flow resistance (mbar·s/cm^3).

Q: Volumetric air flow rate (250 cm^3/s).

ΔP: Pressure drop (mbar).

S: Cross-sectional area of the measurement chamber (cm^2).

ε: Porosity of the fiber plug.

K_0: Kozeny constant (dimensionless).

η: Air viscosity (cN·s/cm^2).

A: Specific surface area (cm^2/cm^3).

Five conditioned fiber specimens (1.2 ± 0.001 g each) were uniformly packed into the measurement chamber to ensure consistent porosity (ε = 0.7–0.9). A constant air flow rate of 15 L/min (250 cm^3/s) was maintained. The Standard Fineness Index (SFI) was then determined.

2.3. Mechanical Characterization

2.3.1. Elementary Fibers

The tensile properties of elementary fibers were measured using the Textechno Favimat device (Figure 5) equipped with a 2 N load cell. Elementary fibers were extracted

and mounted on 3 mg adhesive tabs, to avoid slippage between the jaws. The Favimat system features an integrated unit for the simultaneous measurement of fineness and tensile properties.

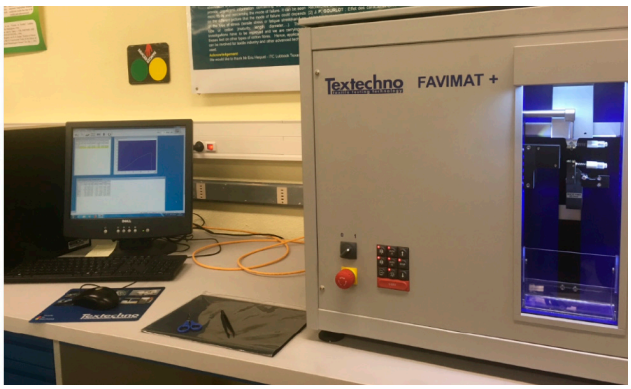


Figure 5. The Textechno Favimat device for elementary fiber tensile testing.

Fibers were reconditioned under standard atmospheric conditions (20 ± 2 °C and 65 ± 2% RH) for 24 h prior to testing. The gauge length was set to 15 mm with a tolerance of ±0.5 mm, and the test speed was 15 mm/min. The following parameters were recorded: fiber fineness (dtex), tenacity (N/tex), specific modulus (N/tex), strain (%), and stress (N).

2.3.2. Technical Fiber Bundles

The mechanical properties of flax technical fiber bundles were evaluated using the MTS testing device (MTS Systems Corporation, Eden Prairie, MN, USA; Model 20/M) with a 100 N load cell. This apparatus applies controlled tensile forces to the fiber until rupture, allowing measurements of stress and strain. The samples were positioned on perforated paper frames (15 mm distance) in which they were glued using a cyanoacrylate adhesive to prevent slippage (Figure 6).

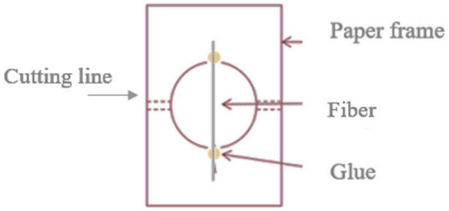


Figure 6. Technical fiber bundles' sample disposition in the MTS device for tensile testing.

The gauge length and test speed were consistent with the protocol used for elementary fiber (15 mm and 15 mm/min, respectively). Special care was taken to apply the glue uniformly at the contact points without penetrating the test region, in order to minimize its impact on the mechanical measurements.

2.3.3. Yarns

Four flax yarns (111.11 tex, 100 tex, 90.9 tex, and 83.33 tex) were spun for this study. Tensile tests were conducted under standard textile testing conditions (ISO 2062), using an MTS testing device (MTS, Model 20/M) equipped with a 100 N load cell. The tests were performed with a gauge length of 500 mm and a crosshead speed of 250 mm/min. A pre-tension of 0.5 cN/tex was applied via the MTS software (0.5 cN/tex)-controlled tensioning system.

To preserve yarn twist during testing, both ends of each yarn were securely clamped to minimize untwisting, and no additional handling was performed between winding and

testing. The measured properties included tenacity (N/tex), specific modulus (N/tex), strain (%), and stress (N).

For each structural scale (elementary fibers, technical bundles, and yarns), a minimum of 15 to 50 replicates were tested to ensure statistical reliability. All experimental data are presented as mean ± standard deviation. Differences in physical and mechanical properties between fiber or yarn groups were evaluated using one-way ANOVA. When significant differences were observed, Tukey's HSD post hoc test was performed for pairwise comparisons. Statistical significance was determined at a 95% confidence level.

3. Results and Discussion

3.1. Physical Characterization

3.1.1. Fiber Length Distribution

The flax fibers analyzed in this study were sampled after the final combing stage (GN4), as this step produced fibers with optimized length and homogeneity for spinning, as confirmed by Almeter analysis (Figure 7).

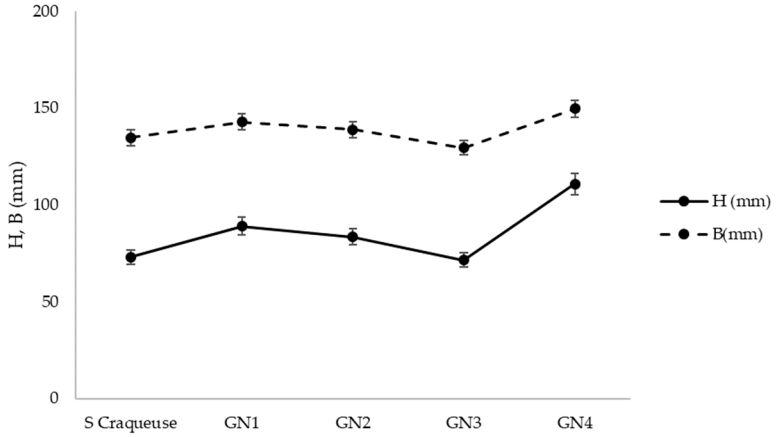


Figure 7. Impact of processing stages on technical flax fiber Almeter length distribution H and B.

Post-GN4 fibers exhibited a mean length (H) of 110.9 mm and an upper quartile length (B) of 149.7 mm, representing a statistically significant increase compared to earlier processing stages ($p < 0.05$). This enhancement resulted from the use of high-density combs at GN4 compared with the previous combings. This comb density preferentially removed residual short fibers, reducing length variability (CvH%: 59.3; CvB%: 37.6) and preserving aligned long fibers, which are critical for tensile load transfer. The evolution of these parameters across all major processing stages is summarized in Table 1.

Table 1. Evolution of Mean Length (H), Upper Quartile Length (B), and Their Coefficients of Variation (CvH%, CvB%) for Technical Flax Fiber Bundles Across Each Preparation Stage (Cracking, GN1–GN4) as Measured by Almeter Analysis.

	Cracking	GN1	GN2	GN3	GN4
H (mm)	73.20	89.10	83.45	71.60	110.9
B (mm)	134.80	142.90	138.85	129.60	149.7
CvH %	91.95	77.80	81.65	90.30	59.3
CvB %	48.15	43.50	45.30	49.70	37.6

Drafting, particularly in multi-stage gill systems used for flax spinning, plays a key role in improving both the length distribution and the effective length of fibers within the sliver. As the sliver undergoes progressive refining, cleavage occurs, leading to an increase

in the average effective fiber length. This enhancement contributes to the production of yarns with improved regularity. Therefore, by focusing on fiber processing at the GN4 stage, direct correlations between fiber-scale characteristics and yarn performance can offer valuable insights for process optimization.

3.1.2. Fineness

To assess the effect of processing on the mean fineness standard index (FSI) of technical flax fiber bundles, FSI values obtained from air flow measurements were compared before and after the final combing stage (GN4). The results indicate a significant decrease in mean FSI, from 49.2 ± 0.44 after the cracking stage to 40.5 ± 0.47 after GN4, representing a reduction of 17.68%. This reduction in FSI reflects the effective removal of coarser fibers during the advanced combing stage, resulting in technical bundles of improved fineness and uniformity. In fact, in flax spinning, drafting improves sliver fineness and uniformity by promoting the cleavage of coarse technical fiber bundles into finer ones. This separation, combined with fiber realignment and redistribution, leads to a thinner, more homogeneous sliver, which is essential for optimized yarn production.

The relationship between fiber length and fineness within technical flax bundles (Table 2) after the final combing stage (GN4) reveals that fineness varies distinctly across the length classes. At shorter fiber lengths (<50 mm), fibers exhibit lower fineness values, likely due to cleavage and fragmentation of bundles into fewer or thinner elements. In the intermediate range (50–150 mm), mean fiber fineness increases, reflecting the presence of more aggregated elementary fibers within technical bundles.

Table 2. Effect of Length Classes on Technical Fiber Bundles Fineness (tex) as Determined by the Vibroscopic Method.

Length Class	Fineness	CV (%)
L > 150 mm	3.30 ± 1.11	3.38
150 mm > L > 50 mm	3.12 ± 1.07	3.42
L < 50 mm	2.63 ± 1.39	5.29

This trend supports the notion that longer fibers tend to retain more bundled structures, as illustrated in Figure 8. Beyond 150 mm, a slight further increase in fineness suggests a possible threshold where fiber aggregation reaches a maximum, beyond which no additional bundling occurs significantly.

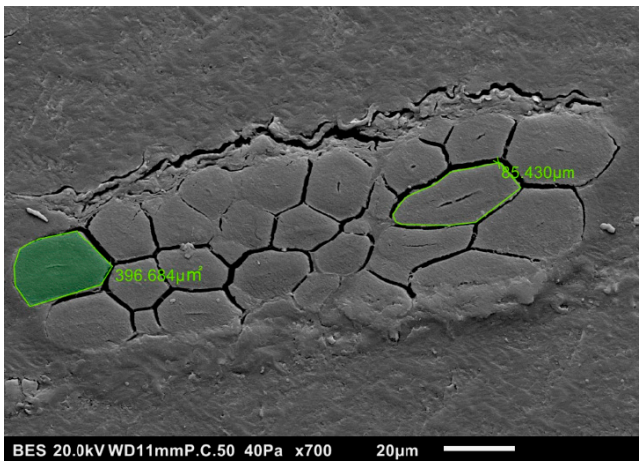


Figure 8. SEM image of elementary flax fiber in technical fiber bundles; 20 kV, ×700.

The combined use of vibroscopic and air flow methods offers a complementary perspective: the vibroscopic technique captures intra-class structural trends, while the air flow method quantifies bulk improvements resulting from processing. Together, these findings demonstrate that advanced combing stages not only improve fiber alignment and length distribution but also refine fiber morphology.

3.2. Mechanical Characterization

3.2.1. Fiber Characterization

The mechanical characterization of flax fibers was conducted across different structural scales, revealing distinct trends related to fiber organization and processing.

Table 3 summarizes the average fineness and specific modulus values for elementary fibers and technical bundles, grouped by length class.

Table 3. Comparative Properties across Fiber Scales and Length Classes.

Group	n	Average Fineness (tex)	Specific Modulus (N/tex)	CV%
Elementary fibers	24	0.22 ± 1.57	1.09 ± 0.62	56.87
Long bundles (>150 mm)	23	3.30 ± 1.11	25.60 ± 8.27	36.80
Medium bundles (50–150 mm)	23	3.12 ± 1.07	20.77 ± 6.88	33.10
Short bundles (<50 mm)	25	2.63 ± 1.39	14.41 ± 9.59	66.60

Elementary fibers, tested using the Favimat device with a gauge length of 15 mm, exhibited the lowest specific modulus (1.09 ± 0.62 N/tex), despite their low fineness (0.22 tex). This reflects the intrinsic mechanical limitations of individual plant cells, where stiffness is primarily governed by the orientation of cellulose microfibrils within the cell walls. The short gauge length was chosen to minimize the influence of macroscopic defects and to isolate the intrinsic response of the microfibrils. Nonetheless, a high degree of variability was observed (CV = 56.87%), indicative of the natural heterogeneity of the fibers and the presence of microstructural weaknesses. The tensile behavior of elementary flax fibers is further illustrated by the representative specific force–strain curves shown in Figure 9. These curves, selected from a broader dataset, capture the range of mechanical responses observed among individual fibers, which vary according to their microstructural integrity. The observed dispersion highlights the intrinsic variability in flax fibers, attributable to differences in cell wall composition, microfibril angle, and internal defects. This mechanical inconsistency is consistent with the high coefficient of variation reported for a specific modulus at this scale.

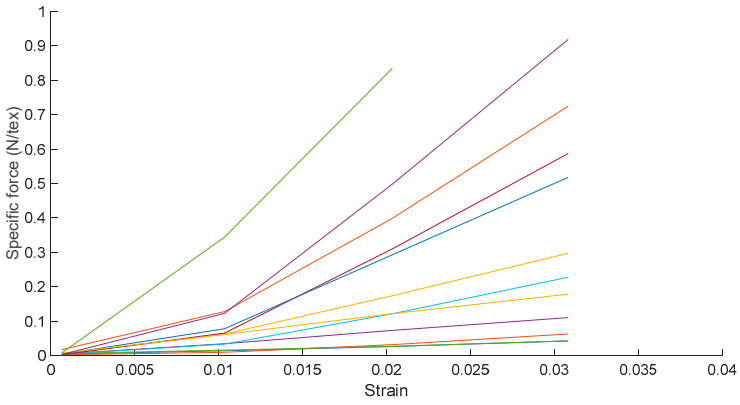


Figure 9. Specific force–strain behavior of elementary flax fibers.

In contrast, technical fiber bundles demonstrated a progressive decrease in mechanical performance with decreasing length, as illustrated in Figure 10a–c.

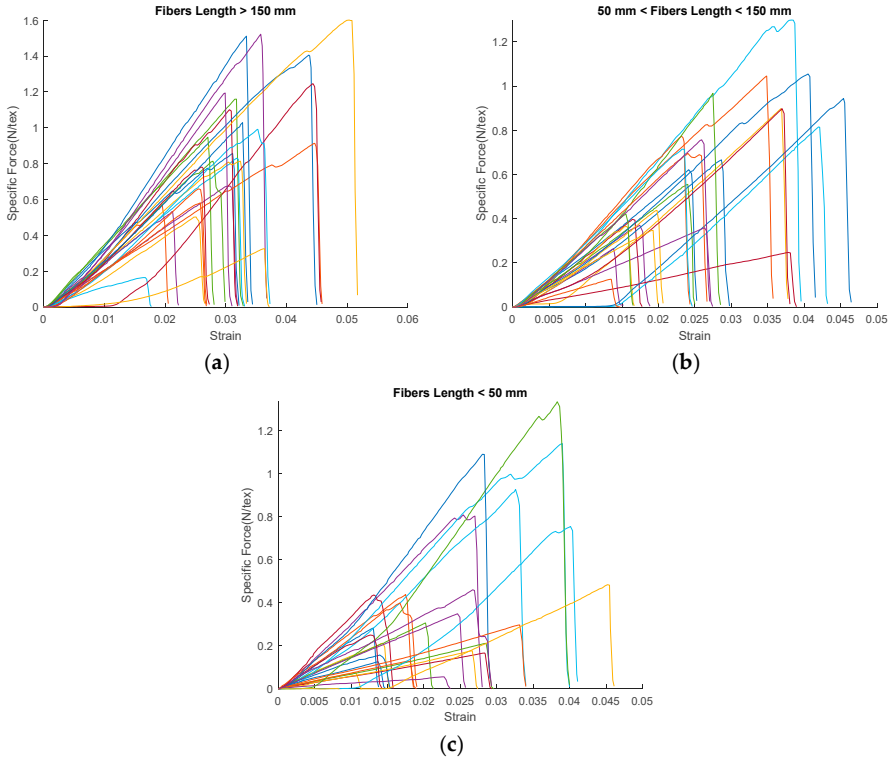


Figure 10. Specific force–strain behavior of technical flax fiber bundles: (**a**) for fiber length more than 150 mm; (**b**) for fiber length between 50 and 150 mm; (**c**) for fiber length less than 50 mm.

To ensure accurate interpretation of the tensile behavior, all specific force–strain curves of technical fiber bundles presented in Figure 10 were corrected to eliminate baseline offsets. Minor deviations from the origin observed in some raw curves were attributed to factors such as adhesive-tab slack, fiber settling under pre-tension, or slight instrument compliance. A post-processing adjustment was applied to align the initial point of each curve with the (0, 0) coordinate. This correction improves the comparability between samples and ensures that mechanical response is evaluated from a common reference point.

Long technical fiber bundles (>150 mm) exhibited the highest specific modulus values (25.60 $\pm$ 8.27 N/tex), while short technical fiber bundles (<50 mm) showed significantly lower moduli (14.41 $\pm$ 9.59 N/tex). Medium-length bundles (50–150 mm) displayed intermediate mechanical performance with an average specific modulus of 20.77 $\pm$ 6.88 N/tex. This category also showed a relatively lower coefficient of variation (33.10%), indicating more uniform fiber organization and fewer internal defects compared to shorter bundles. The observed mechanical behavior suggests improved load transfer and reduced inter-fiber slippage as bundle length increases, contributing to enhanced stiffness.

These findings highlight the importance of fiber length on the mechanical properties of flax bundles and reveal a progressive transition in modulus values across the different length scales.

Statistical analysis using one-way ANOVA confirmed significant differences in specific modulus across groups (F = 45.54, $p < 0.001$; Table 4).

Table 4. One-Way ANOVA Results for Specific Modulus Across Fiber Groups.

Source	df	Sum of Squares	Mean Square	F-Value	*p*-Value
Between groups	3	7032.92	2344.31	45.54	<0.001
Within group	91	4684.99	51.48	-	-
Total	94	11,717.91	-	-	-

Post hoc Tukey tests revealed that all fiber types differed significantly from one other ($p < 0.001$; Table 5), except for the comparison between medium and short bundles ($p = 0.775$; Table 5). Long bundles exhibited a significantly higher modulus than both medium bundles ($p = 0.007$; Table 5) and short bundles ($p < 0.001$; Table 5).

Table 5. Post Hoc Tukey HSD Pairwise Comparisons for Specific Modulus (N/tex).

Comparison	Mean Difference (N/tex)	*p*-Value	Significance
Long vs. Medium bundles	7.06	0.007	Significant
Long vs. Short bundles	9.04	<0.001	Significant
Medium vs. Short bundles	1.98	0.775	Not significant

These results highlight the impact of flax fiber structure on mechanical properties. While elementary fibers exhibit behavior dominated by fiber nanoscale composition and fiber orientation, technical bundles introduce additional factors such as inter-fiber bonding and alignment.

The high variability observed in short bundles (CV = 66.60%), as shown in Table 4, suggests uneven processing outcomes, potentially due to incomplete separation of the fibers in the previous stages. Conversely, long bundles (>150 mm) exhibited improved uniformity (CV = 36.80%), reflecting the efficiency of the combing stage (GN4) in aligning fibers and removing structural defects. This supports the industrial focus on using longer fibers for high-performance yarns, where mechanical integrity is critical.

3.2.2. Yarn Characterization

The tensile behavior of the four flax yarns (111.11 tex, 100 tex, 90.9 tex, and 83.33 tex) is presented in Figure 11, which displays the specific force (N/tex) as a function of strain.

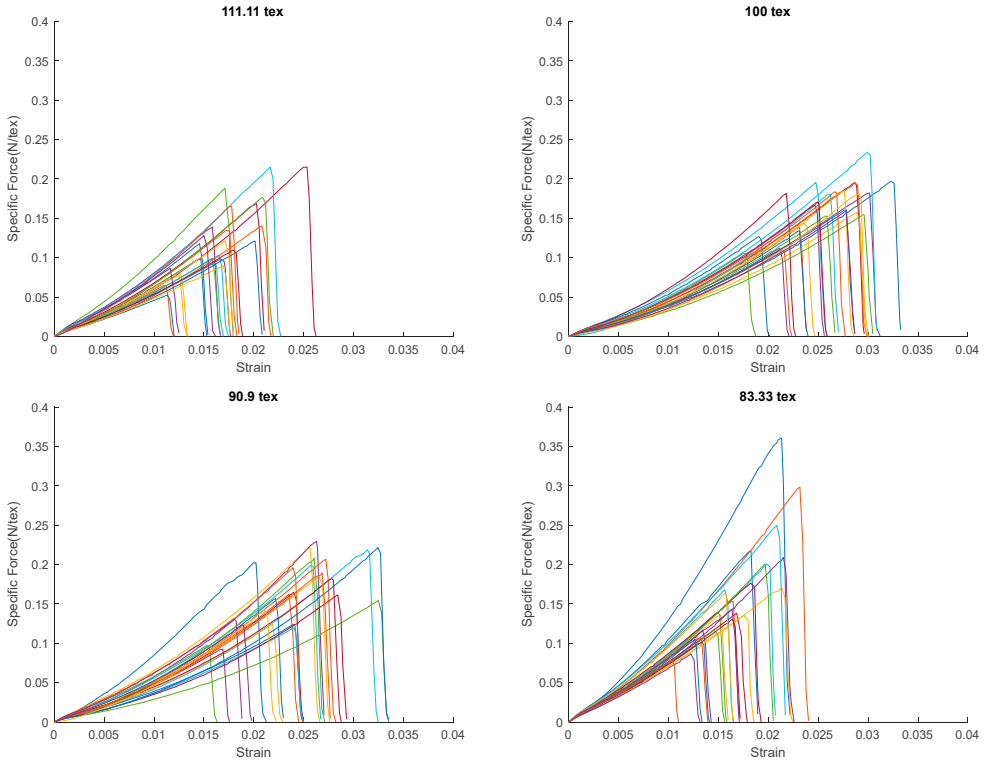


Figure 11. Specific force–strain behavior of technical flax for flax yarns of count 111.11 tex, 100 tex, 90.9 tex, and 83.33 tex.

All yarns exhibit characteristic linear elastic behavior at low strain, followed by a progressive failure typical of a multifilament structure, indicative of the gradual breakage and slippage of fibers within the yarn structure.

The mechanical properties extracted from these curves are summarized in Table 6.

Table 6. Mechanical Properties of Flax Yarns.

Yarn Count (tex)	Twist (t/m)	Tenacity (N/tex)	Specific Modulus (N/tex)	Avg, Technical Fibers/Section	Avg, Elementary Fibers/Section	CV% Yarn Regularity
111.11	352	11.00 ± 1.25 35.67 CV%	5.53 ± 1.25 24.52 CV%	37	505	37.3
100	383	16.00 ± 0.65 17.68 CV%	5.26 ± 0.65 13.35 CV%	33	455	35.95
90.9	398	17.12 ± 0.96 24.70 CV%	5.68 ± 0.96 18.79 CV%	30	413	35.89
83.33	416	17.14 ± 1.69 34.00 CV%	7.32 ± 1.69 28.97 CV%	28	379	34.74

The coefficient of variation (CV%) for yarn regularity remains relatively high (34–37%), reflecting the inherent variability of flax fibers. Nevertheless, a slight decrease in CV% for the yarn regularity with decreasing yarn count suggests that finer yarns benefit from improved homogeneity and more efficient spinning conditions. As the yarn count decreases, meaning the yarn becomes finer, both the tenacity and the specific modulus increase. For example, the finest yarn (83.33 tex) exhibits the highest specific modulus (7.32 ± 1.69 N/tex) and tenacity (17.14 ± 1.69 N/tex), while the coarsest yarn (111.11 tex) shows the lowest values (5.53 ± 1.25 N/tex and 11.00 ± 1.25 N/tex, respectively). Higher twist and improved fiber alignment are coherent with this evolution. The mean specific modulus increases with yarn fineness, although the variability (expressed as standard deviation and CV%) remains significant, particularly for coarser yarns.

One-way ANOVA confirmed that yarn count significantly affects both specific modulus ($F(3.96) = 15.89$, $p < 0.001$) and maximum force ($F(3.96) = 7.45$, $p < 0.001$) (Table 7). Post hoc Tukey HSD tests further clarified these differences (Table 8).

Table 7. One Way ANOVA Results for Specific Modulus Across Yarn Groups.

Source	df	Sum of Squares	Mean Square	F-Value	*p*-Value
Between groups	3	69.53	23.18	15.89	<0.001
Within group	96	139.98	1.46	-	-
Total	99	209.51	-	-	-

Table 8. Post Hoc Tukey HSD Pairwise Comparisons for Specific Modulus (N/tex).

Comparison	Mean Difference (N/tex)	*p*-Value	Significance
83.33 tex vs. 111.11 tex	+1.78	<0.001	Significant
83.33 tex vs. 100 tex	+2.12	<0.001	Significant
83.33 tex vs. 100 tex	+1.73	<0.001	Significant
100 tex vs. 111.11 tex	+0.05	0.775	Not significant
100 tex vs. 100 tex	+0.38	0.102	Not significant
111.11 tex vs. 100 tex	+0.34	0.143	Not significant

The analysis reveals that the finest yarn (83.33 tex) has a significantly higher specific modulus compared to all other yarn counts ($p < 0.001$). This is likely due to better fiber alignment and lower defect density. However, no statistically significant differences were found between the 90.9 tex, 100 tex, and 111.11 tex yarn counts ($p > 0.05$), suggesting similar mechanical performance among these coarser yarn types.

This improvement is attributed to a combination of higher twist, improved packing, and enhanced fiber alignment within the yarn structure. Although direct microstructural measurements such as SEM imaging or misalignment angle distribution were not performed in this study, previous work has demonstrated the central role of fiber orientation in determining the tensile behavior of natural fiber yarns and composites. For instance, studies [20,21] have shown that yarns with lower misalignment angles exhibit higher stiffness, owing to efficient load transfer between fibers.

The mechanical characterization of flax yarns demonstrates that optimizing fineness and twist leads to a higher specific modulus and tenacity, primarily due to improved fiber alignment and packing. However, the inherent variability of flax fibers remains a limiting factor for yarn regularity and strength consistency.

The coefficients of variation observed in this study are characteristic of the natural heterogeneity inherent to flax fibers. Variability in cell wall composition, microfibril orientation, and the presence of micro-defects significantly contribute to the dispersion of mechanical properties at the elementary fiber scale. At the yarn level, regularity reflects not only this intrinsic fiber variability but also the efficiency of fiber alignment and control during the spinning process. Although the final combing stage (GN4) improves uniformity by removing shorter and damaged fibers and enhancing alignment, a certain degree of variability is unavoidable due to the natural origin of the material. These findings highlight the inherent challenge of achieving consistent mechanical performance in natural fiber-based products.

Future improvements may arise from more refined fiber selection, optimized processing steps, and increased sample sizes to better capture and control this variability.

4. Conclusions

This study provides a comprehensive multiscale characterization of flax fibers, from elementary fibers to technical bundles and finally to yarns, highlighting how structural features at each scale influence the mechanical properties of a linear textile material. Our results demonstrate a progressive decline in specific modulus and tenacity from elementary fibers through technical bundles to yarns. At the elementary fiber scale, fibers exhibited the highest specific modulus but also the greatest variability, reflecting inherent microstructural heterogeneity. At the level of technical fiber bundles, mechanical homogeneity and intermediate properties improved, with longer bundles (>150 mm) outperforming shorter ones due to enhanced fiber alignment and reduced defect density. These results highlight the critical role of fiber length retention and alignment at this intermediate scale.

At the yarn scale, the findings confirm that optimizing yarn fineness and twist contributes to enhanced mechanical performance, primarily by improving fiber packing and alignment within the yarn structure. Nevertheless, the natural variability of flax fibers remains a major source of mechanical scatter, especially in coarser yarns. Statistical analysis (ANOVA and post hoc Tukey tests) confirmed that the finest yarns (83.33 tex) exhibited significantly better mechanical properties, with an approximately 32% increase in specific modulus and 28% increase in tenacity compared to the coarsest yarn (111.11 tex). Adding to this, the high coefficients of variation (CV%) observed, especially in coarser yarns, reflect the intrinsic variability of natural fibers.

Overall, at each structural scale, mechanical performance was influenced not only by structural integrity but also by the degree of fiber alignment. This observation is consistent with previous studies [4,7,10] showing that increased misalignment angles are associated with a decrease in specific modulus by up to 30%, confirming the critical role of fiber orientation in determining mechanical performance.

Although the individual processing stages used are well established, the novelty of this work lies in its integrated, multiscale analysis of mechanical behavior across the fiber hierarchy. The dry spinning process was carefully selected and optimized to preserve structural integrity and enhance alignment. Thus, it helps by providing a controlled framework for investigating the influence of processing on final yarn performance.

These findings reinforce the importance of advanced fiber selection, processing, and spinning protocols to maximize mechanical performance and minimize variability in flax-based textiles.

Future work will focus on refining the combing and drafting stages, with particular attention given to integrating fiber regularity control throughout the processing chain. In parallel, further research will investigate the direct relationship between spinning parameters and fiber regularity, thereby complementing the present study and deepening the understanding of flax fiber processing–performance interactions.

Our results provide actionable insights into both industrial-scale processing and the development of sustainable flax-based materials. They align with the growing consensus in the literature regarding the critical influence of fiber structure and processing conditions on the performance of natural fiber composites and textiles.

Author Contributions: W.M.: methodology, software, formal analysis, investigation, writing—original draft, and visualization; O.H.: methodology, validation, resources, and review and editing. All authors have read and agreed to the published version of the manuscript.

Funding: This research received no external funding.

Data Availability Statement: The original contributions presented in the study are included in the article, further inquiries can be directed to the corresponding authors.

Conflicts of Interest: The authors declare no conflicts of interest. The funders had no role in the design of this study; in the collection, analyses, or interpretation of data; in the writing of the manuscript; or in the decision to publish the results.

References

1. Elfaleh, I.; Abbassi, F.; Habibi, M.; Ahmad, F.; Guedri, M.; Nasri, M.; Garnier, C. A comprehensive review of natural fibers and their composites: An eco-friendly alternative to conventional materials. *Results Eng.* **2023**, *19*, 101271. [CrossRef]
2. Baley, C.; Le Duigou, A.; Morvan, C.; Bourmaud, A. Tensile properties of flax fibers. In *Handbook of Properties of Textile and Technical Fibres*; Miao, M., Ed.; Woodhead Publishing: Cambridge, UK, 2018; pp. 275–300.
3. Zhu, S.; Xie, J.; Sun, Q.; Zhang, Z.; Wan, J.; Zhou, Z.; Lu, J.; Chen, J.; Xu, J.; Chen, K.; et al. Recent advances on bast fiber composites: Engineering innovations, applications and perspectives. *Compos. Part B Eng.* **2024**, *284*, 111738. [CrossRef]
4. Aldroubi, S.; Kasal, B.; Yan, L.; Bachtiar, E.V. Multi-scale investigation of morphological, physical and tensile properties of flax single fiber, yarn and unidirectional fabric. *Compos. Part B Eng.* **2023**, *259*, 110732. [CrossRef]
5. Omrani, F.; Wang, P.; Soulat, D.; Ferreira, M. Mechanical properties of flax-fibre-reinforced preforms and composites: Influence of the type of yarns on multi-scale characterisations. *Compos. Part A Appl. Sci. Manuf.* **2017**, *93*, 72–81. [CrossRef]
6. Ragoubi, M.; Lecoublet, M.; Khennache, M.; Poilane, C.; Leblanc, N. Multi Scale Analysis of the Retting and Process Effect on the Properties of Flax Bio-Based Composites. *Polymers* **2023**, *15*, 2531. [CrossRef] [PubMed]
7. Thomason, J.; Carruthers, J.; Kelly, J.; Johnson, G. Fibre cross-section determination and variability in sisal and flax and its effects on fibre performance characterisation. *Compos. Sci. Technol.* **2011**, *71*, 1008–1015. [CrossRef]
8. Blervacq, A.-S.; Moreau, M.; Duputié, A.; De Waele, I.; Duponchel, L.; Hawkins, S. Raman spectroscopy mapping of changes in the organization and relative quantities of cell wall polymers in bast fiber cell walls of flax plants exposed to gravitropic stress. *Front. Plant Sci.* **2022**, *13*, 976351. [CrossRef] [PubMed]
9. Angulu, M.; Gusovius, H.-J. Retting of Bast Fiber Crops Like Hemp and Flax—A Review for Classification of Procedures. *Fibers* **2024**, *12*, 28. [CrossRef]
10. Goudenhooft, C.; Melelli, A.; Durand, S.; Falourd, X.; Le-Bot, L.; Morgillo, L.; Gaballah, S.; Cortopassi, R.; Quiles, A.; Shah, D.U.; et al. Comparison of kink-band structures and specificities of cell wall polysaccharides in modern and ancient flax fibres. *Carbohydr. Polym.* **2024**, *344*, 122526. [CrossRef] [PubMed]

11. Styles, J. Flax, hemp, ramie and jute: The bast fibres. In *Textiles and Clothing Along the Silk Roads: Thematic Collection of the Cultural Exchanges Along the Silk Roads*; UNESCO: Paris, France, 2022; Volume 1, p. 45.
12. Zimniewska, M. Hemp Fibre Properties and Processing Target Textile: A Review. *Materials* **2022**, *15*, 1901. [CrossRef] [PubMed]
13. Koksharov, S.; Aleeva, S.; Lepilova, O. Nanostructural Biochemical Modification of Flax Fiber in the Processes of Its Preparation For Spinning. *Autex Res. J.* **2015**, *15*, 215–225. [CrossRef]
14. Das, S.C.; La Rosa, A.D.; Goutianos, S.; Grammatikos, S.A. Flax fibers, their composites and application. In *Plant Fibers, Their Composites, and Applications*; Jawaid, M., Khan, M.M., Eds.; Woodhead Publishing: Cambridge, UK, 2022; pp. 209–232.
15. Wang, J.; Li, Y.; Li, Q.; Long, Y.; Yu, T.; Li, Z. Evolution of stiffness in flax yarn within flax fiber reinforced composites during moisture absorption. *Compos. Part B Eng.* **2023**, *268*, 111096. [CrossRef]
16. Green, J.; Liu, X.; Yin, R. A Brief Review of Hemp Fiber Length Measurement Techniques. *Fibers* **2024**, *12*, 93. [CrossRef]
17. *ASTM D1440-90*; Standard Test Method of Length and Length Distribution of Cotton Fibers (Array Method). ASTM International: West Conshohocken, PA, USA, 1997.
18. Harzallah, O.; Dre, J.-Y. *Macro and Micro Characterization of Biopolymers: Case of Cotton Fibre*; InTech: Rijeka, Croatia, 2011.
19. Mahjoub, W.; Harzallah, O.; Gourlot, J.-P.; Drean, J.-Y. Modelling the creep behavior of Gossypium hirsutum cotton fibers based on their physical and mechanical properties. *Ind. Crop. Prod.* **2023**, *203*, 117223. [CrossRef]
20. Richely, E.; Nuez, L.; Pérez, J.; Rivard, C.; Baley, C.; Bourmaud, A.; Guessasma, S.; Beaugrand, J. Influence of defects on the tensile behaviour of flax fibres: Cellulose microfibrils evolution by synchrotron X-ray diffraction and finite element modelling. *Compos. Part C Open Access* **2022**, *9*, 100300. [CrossRef]
21. Baley, C. Analysis of the flax fibres tensile behaviour and analysis of the tensile stiffness increase. *Compos. Part A Appl. Sci. Manuf.* **2002**, *33*, 939–948. [CrossRef]

Disclaimer/Publisher's Note: The statements, opinions and data contained in all publications are solely those of the individual author(s) and contributor(s) and not of MDPI and/or the editor(s). MDPI and/or the editor(s) disclaim responsibility for any injury to people or property resulting from any ideas, methods, instructions or products referred to in the content.